MRMS QPE Performance East of the Rockies during the 2014 Warm Season

STEPHEN B. COCKS

Cooperative Institute for Mesoscale Meteorological Studies, University of Oklahoma, and NOAA/OAR/National Severe Storms Laboratory, Norman, Oklahoma

JIAN ZHANG

NOAA/OAR/National Severe Storms Laboratory, Norman, Oklahoma

STEVEN M. MARTINAITIS, YOUCUN QI, AND BRIAN KANEY

Cooperative Institute for Mesoscale Meteorological Studies, University of Oklahoma, and NOAA/OAR/National Severe Storms Laboratory, Norman, Oklahoma

KENNETH HOWARD

NOAA/OAR/National Severe Storms Laboratory, Norman, Oklahoma

(Manuscript received 27 July 2016, in final form 15 November 2016)

ABSTRACT

Multi-Radar Multi-Sensor (MRMS) quantitative precipitation estimation (QPE) radar only (Q3RAD), Q3RAD local gauge corrected (Q3gc), dual polarization (Dual Pol), legacy Precipitation Processing System (PPS), and National Centers for Environmental Prediction (NCEP) stage IV product performance were evaluated for data collected east of the Rockies during the 2014 warm season. For over 22 000 radar QPE–gauge data pairs, Q3RAD had a higher correlation coefficient (0.85) and a lower mean absolute error (9.4 mm) than the Dual Pol (0.83 and 10.5 mm, respectively) and PPS (0.79 and 10.8 mm, respectively). Q3RAD performed best when the radar beam sampled precipitation within or above the melting layer because of its use of a reflectivity mosaic corrected for brightband contamination. Both NCEP stage IV and Q3gc showed improvement over the radar-only QPEs; while stage IV exhibited the lower errors, the performance of Q3gc was remarkable considering the estimates were automatically generated in near–real time. Regional analysis indicated Q3RAD outperformed Dual Pol and PPS over the southern plains, Southeast/mid-Atlantic, and Northeast. Over the northern United States, Q3RAD had a higher wet bias below the melting layer than both Dual Pol and PPS; within and above the melting layer, Q3RAD exhibited the lowest errors. The Q3RAD wet bias was likely due to MRMS's overestimation of tropical rain areas in continental regions and applying a high yield reflectivity–rain-rate relationship. An adjustment based on precipitation climatology reduced the wet bias errors by ~22% and will be implemented in the operational MRMS in the fall of 2016.

1. Introduction

Multi-Radar Multi-Sensor (MRMS) quantitative precipitation estimation (QPE) products have been produced for National Weather Service (NWS) operations since September 2014 (Zhang et al. 2014, 2016). As part of a continuing effort to improve MRMS products, extensive evaluations have been conducted for the various regions across the United States as well as the different seasons. A recent cool season QPE assessment east of the Rocky Mountains highlighted radar precipitation estimate challenges related to brightband contamination and radar beam overshoot of shallow precipitation systems (Cocks et al. 2016). These challenges are especially relevant for single-radar-generated QPE; however, a mosaicked product, such as the MRMS radar-only QPE (Q3RAD), can mitigate radar beam overshoot primarily via the use of multiple radar inputs for a given grid point. Further, the application of a

Corresponding author e-mail: Stephen B. Cocks, stephen.cocks@noaa.gov

DOI: 10.1175/JHM-D-16-0179.1

vertical profile of reflectivity (VPR) correction in MRMS (Zhang and Qi 2010) can mitigate melting layer effects that were clearly illustrated via cool season performance comparisons between Q3RAD and mosaicked dual polarization (Dual Pol) estimates, which lacked an effective brightband correction (Cocks et al. 2016).

During the warm season, both radar beam overshoot and brightband contamination are less common as deep convection and higher freezing levels are more prevalent. The logical follow-up to a cool season study was to assess QPE performance east of the Rockies for the 2014 warm season to document strengths and weaknesses, the purpose of this study. As many previous studies have documented, radar QPE assessments involve intercomparisons of radar precipitation estimates to rain gauge accumulations, and a number of limitations must be considered (Wilson and Brandes 1979; Krajewski et al. 2010). Ground clutter, blockage, and nonmeteorological echoes contaminating the lower-elevation scans, partial beam filling effects and increased sample volumes at greater distances (Steiner et al. 1999; Zhang et al. 2012), beam overshoot and brightbanding effects (Smith et al. 1996; Zhang and Qi 2010), improper calibration, signal attenuation (Doviak and Zrnić 2006; Rinehart 2010), and the use of improper reflectivity–rain-rate (Z–R) relationships (Wilson and Brandes 1979; Steiner et al. 1999) all can significantly affect radar-derived precipitation estimates. On the other hand, blockages and poor site placement (Sieck et al. 2007; Fiebrich et al. 2010), undercatch due to wind (Wilson and Brandes 1979; Sieck et al. 2007), power outages preventing data transmission (Martinaitis 2008), mechanical malfunctions, and telemetry and transmission problems (Groisman and Legates 1994; Marzen and Fuelberg 2005; Kim et al. 2009) can contribute to gauge errors. Further, the typical surface area volume of a radar pixel and a rain gauge can differ by as much as eight orders of magnitude (Droegemeier et al. 2000).

With these considerations in mind, single-radar QPEs along with mosaicked QPEs from the MRMS system were assessed for precipitation events observed by 55 radars on 59 calendar days between 29 March and 28 September 2014. These precipitation estimate performances were compared to the forecaster quality-controlled National Centers for Environmental Prediction (NCEP) stage IV precipitation estimates. Unlike the previous cool season QPE study, this assessment was made in reference to the radar location, that is, mosaicked and single-radar QPE were compared for each radar location out to a distance of 230 km. The reason was to determine if the advantages of a QPE mosaic with a brightband correction for reflectivity when compared with single-radar QPE were still relevant during warm season precipitation events. This paper is organized as follows: section 2 covers the data methodology, section 3 covers the statistical results for the entire domain east of the Rockies, section 4 discusses the statistical results for five predefined geographical regions, and section 5 is a summary.

2. Data, methodology, and quality-control measures

The criteria for choosing precipitation events for evaluation was whether significant areas received rain totals ≥25.4 mm (1.00 in.) and whether all five precipitation products [MRMS, Dual Pol, Precipitation Processing System (PPS), Q3RAD local gauge corrected (Q3gc), and stage IV] data were available within the MRMS archive system. For the evaluated precipitation events, upper-air, numerical model, and radar data combined with radar rainfall and gauge totals were evaluated for 24-h periods ending at 1200 UTC. Hourly and 24-h radar-derived estimates and gauge accumulations were compared at corresponding grid points (henceforth called R/G pairs). Gauge data consisted of 24-h precipitation data from the Community Collaborative Rain, Hail and Snow Network (CoCoRaHS) and hourly data from Hydrometeorological Automated Data System (HADS).

The following precipitation estimate products were evaluated: MRMS Q3RAD, Q3gc, NCEP stage IV, single-radar Dual Pol, and single-radar legacy PPS. MRMS Q3RAD estimates are derived from quality-controlled reflectivity mosaics corrected for brightband contamination. Multiple Z–R relationships were applied according to the MRMS surface precipitation type at each grid cell based on vertical profiles of reflectivity and environmental data (Zhang et al. 2016). Q3gc estimates are Q3RAD estimates locally adjusted by hourly HADS gauge data using an inverse distance weighting (IDW) scheme. A description of these two MRMS products can be found in Cocks et al. (2016) and Zhang et al. (2011, 2016).

The 24-h NCEP stage IV data were the mosaic of continental U.S. River Forecast Center (RFC) estimates that utilized manual quality control (QC) of radar, satellite, and gauge data. Nelson et al. (2016) provided a summary of the process involved in making NCEP stage IV estimates. However, it is important to note that that the radar portions of the stage IV analysis were not always comprised of the same radar-only QPE product (e.g., PPS). For example, RFCs may use PPS, Q3RAD, satellite precipitation estimates, a gauge-only analysis, or, more recently, Dual Pol or even a combination in

order to maximize the accuracy of the analysis (G. Story and E. Jones 2016, personal communication; Wardlow et al. 2012). Hence, different sections of the contiguous U.S. stage IV analysis may incorporate different radar-only QPEs, albeit gauge corrected. Nonetheless, the forecaster QC of the stage IV analysis makes it the standard by which the QPEs in this study may be measured against.

The Dual Pol QPE algorithm utilizes a fuzzy-logic-based radar echo classifier, the hybrid-hydrometeorological classification algorithm (HHC), to assign rain rates based upon specific differential phase K_{DP}, differential reflectivity Z_{DR}, and reflectivity Z. A more comprehensive description can be found in Giangrande and Ryzhkov (2008) and Berkowitz et al. (2013). The legacy PPS estimates utilize a single Z–R relation for the radar's entire field of view for each volume scan, and the Z–R relation can be changed when deemed necessary by the operational forecaster. A more detailed description of the PPS algorithm can be found in Fulton et al. (1998).

Comparisons between a mosaic and single-radar QPE data usually involve resolution and coordinate system differences, and this was the case for this study. Single-radar QPE was in polar coordinates while Q3RAD, Q3gc, and stage IV QPE were in Cartesian coordinates. Further, there are resolution differences among the different products. For example, the NCEP stage IV QPE is distributed in 4 km × 4 km resolution in Cartesian coordinates. To better match the 1 km × 1 km resolution of Q3RAD and Q3gc, the NCEP stage IV data have been remapped, using a nearest neighbor approach, to 1 km × 1 km Cartesian grids for over 5 years. Operational PPS estimates were available in 4 km × 1° resolution, coarser than desired for comparison studies. Similar to what was done with stage IV data, a higher-resolution (1 km × 1°) version of PPS was generated within MRMS by using the Z–R relations and the Digital Hybrid Scan Reflectivity (DHR) data found in Weather Surveillance Radar-1988 Doppler (WSR-88D) level-III data. Operational Dual Pol precipitation QPE fields, also available in WSR-88D level-III data, had a higher resolution of 0.25 km × 1°. Rather than attempt a lengthy regridding project for the Dual Pol QPE fields, a simple test was first conducted. A comparison was made between R/G pairs for single-radar Dual Pol (0.25 km × 1°, polar coordinates) QPE to the same pairs transformed to 1 km × 1 km Cartesian coordinates to determine if the resolution and coordinate differences significantly masked any performance trends. The R/G pairs, a total of 4693, were collected from 12 radars for over 50 precipitation events. The scatterplots, shown in Fig. 1, were quite similar. While there were some individual R/G pairs from the higher-resolution data that showed some significant differences from the lower-resolution data, because of the location of the gauge along a very tight QPE gradient, the overall difference between the two samples was small, with only a slightly higher overestimate bias ratio for the higher-resolution data (Fig. 1). The root-mean-square error (RMSE) and mean absolute error (MAE) differences between the higher-resolution polar coordinate Dual Pol data and that in lower resolution in Cartesian coordinates were <1 mm. Differences in radar-to-gauge bias ratios were only 0.05 while the correlation coefficients were identical. This test provided confidence in making the comparisons between the mosaicked QPE in Cartesian coordinates and the single-radar QPE in polar coordinates when the data sample was sufficiently large.

Precipitation estimates were compared to independent 24-h accumulations from CoCoRaHS gauges, which, from experience, were more consistent and suitable. Further, these gauges serve as an independent check for the MRMS Q3gc estimates, as only hourly HADS gauges are used to correct the radar-only QPE. As a minimal QC measure, both the radar-based QPEs and the CoCoRaHS gauges were required to be ≥2.5 mm (0.01 in.) before including the R/G pair into the analysis. To compare performances between mosaic estimates and the single-radar QPEs, data were evaluated for R/G pairs with a distance ≤230 km of the radar location, the maximum range that precipitation estimates were created by the Dual Pol and PPS QPE algorithms.

Performance statistics were stratified by 24-h CoCoRaHS gauge totals, by distance from the radar, and by the position of the radar beam with respect to the melting layer. Dual Pol correlation coefficient (CC) data, which are the correlation between the horizontal and vertical power at zero time lag, were used to differentiate regions of pure rain and mixed phase hydrometeors. In this data, the melting layer was generally discerned as a ring of lower CC values, generally <0.97, as precipitation events passed through a radar's field of view (Kumjian 2013). Hourly inspection of CC data for each precipitation event provided an approximation of the bottom of the melting layer and its minimum distance from the radar during a 24-h period. If the melting layer was difficult to discern, nearby rawinsonde or model data were used. The R/G pairs were then stratified into regions where precipitation was generally below or within the melting layer. With the exception of the early warm season cases, inspection of precipitation events indicated that the top of the melting layer was often located at distances greater than 180 km from the radar, a region where QPE underestimates were a little

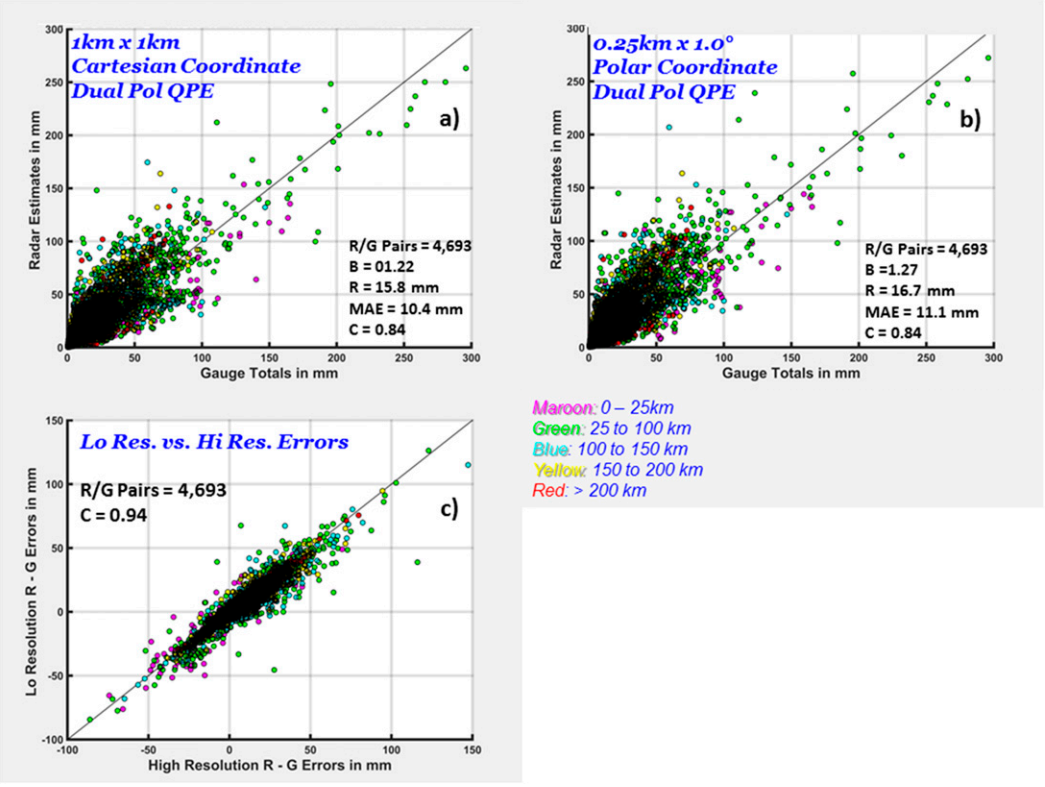

FIG. 1. Comparison between (a) 1 km × 1 km Cartesian and (b) 0.25 km × 1.0° polar coordinate Dual Pol estimates using matched *R*/*G* pairs. (c) Plot of low- vs high-resolution errors. In the legend, *B*, *R*, MAE, and *C* stand for radar-to-gauge bias ratio, RMSE, MAE, and CC, respectively.

more prevalent. As an approximation, the authors considered distances >200 km as the region where a significant portion of the radar beam was sampling within the ice region. Hence, this distance was used to evaluate the QPE impacts when the radar beam was generally above the melting layer.

Statistical measures used in the evaluations were mean bias ratio, defined as the ratio of the gauge total to radar estimate, RMSE, MAE, and correlation coefficient. Hourly HADS data were quality controlled with the same measures used in Cocks et al. (2016) and then used to diagnose error trends as well as QPE impacts after algorithm adjustments. QPE evaluations were evaluated for the entire area east of the Rockies as well as for five subregions: the southern plains, the northern and central plains, the Great Lakes/Midwest, the Northeast, and the Southeast/mid-Atlantic (Fig. 2).

3. Statistical analysis and results for all *R*/*G* pairs east of the Rockies

Figures 3a–c show the scatterplots for all *R*/*G* pairs east of the Rockies. The Dual Pol (PPS) RMSEs were 1.1 mm (2.1 mm) higher than Q3RAD; Dual Pol (PPS) MAE were 1.1 mm (1.4 mm) higher than Q3RAD. Q3RAD exhibited a higher CC than Dual Pol (0.85 vs 0.83), which was most notable for gauge totals less than 125.0 mm; for higher gauge totals Q3RAD had slightly more scatter than Dual Pol. Gauge-to-radar estimate bias ratios indicated Q3RAD had a slightly higher tendency to overestimate precipitation than Dual Pol (0.93 vs 0.96). Both products exhibited a significantly better overall performance than PPS, which exhibited an underestimate bias ratio (1.13) and lower correlation (0.78). Overall, Dual Pol QPE performance was much better than seen in the previous cool season (Cocks et al. 2016). This was expected because of the deeper vertical extent of precipitation systems and less brightband contamination of radar reflectivity due to the higher freezing levels during the warm season. Figures 3d and 3e showed a performance comparison between MRMS Q3gc and the NCEP stage IV QPE. The forecaster quality-controlled stage IV data had significantly lower RMSE (10.7 mm) and MAE (6.5 mm) than MRMS Q3gc (12.0 and 7.2 mm, respectively); however, Q3gc and stage IV exhibited essentially the same mean bias ratio and similar correlation coefficients. While the NCEP stage IV scatterplots were better behaved with less variability than MRMS Q3gc, it

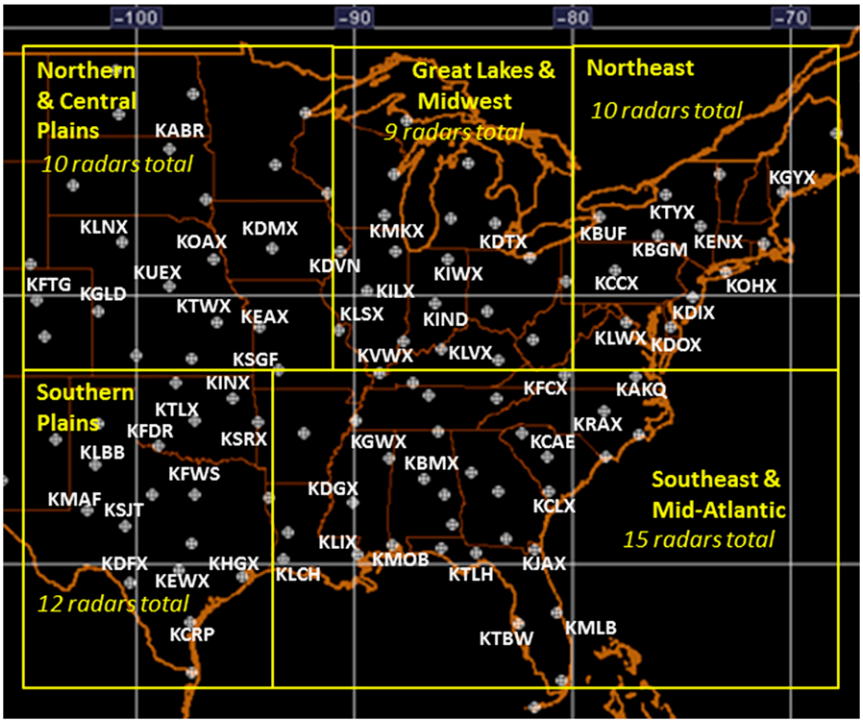

FIG. 2. Regions and radars used for 2014 warm season evaluation.

was still remarkable how competitive Q3gc estimates were considering it is an automated, quality-controlled product available hourly versus the manual processes and potential delays associated with stage IV.

Table 1 shows the Q3RAD, Dual Pol, PPS, Q3gc, and NCEP stage IV statistical measures for R/G pairs $\leq$230 km stratified by the following 24-h gauge totals: 1) light precipitation category with gauge totals $<$12.7 mm (0.50 in.), 2) moderate with totals $\geq$12.7 mm (0.50 in.) and $\leq$38.1 mm (1.50 in.), 3) moderately high with totals $>$38.1 mm (1.50 in.) and $\leq$101.6 mm (4.00 in.), and 4) high with totals $>$101.6 mm (4.00 in.). All of the products exhibited a significant overestimate trend and similar RMSE and MAE values for the light precipitation category, with stage IV and Q3gc having the lowest errors. The overestimate bias was likely due to a combination of the evaporation of precipitation before reaching the ground and the gauge wetting orifice effect, where small droplets may dry off before a sufficient number coalesce and run into the gauge bucket. For moderate precipitation totals, Q3RAD and Dual Pol continued to exhibit more of an overestimate bias than the other products, although the magnitude was less than seen in the previous category. Stage IV had the lowest RMSE and MAE followed by Q3gc, Q3RAD, PPS, and Dual Pol.

For the moderately high and high precipitation amount categories, both stage IV and Q3gc continued to exhibit lower errors than the radar-only products (Q3RAD, Dual Pol, and PPS). Stage IV RMSE and MAE values were 34% less than the next best radar-only estimate (Q3RAD). All of the products exhibited a significant underestimate bias, with the worst being PPS. Considering the potential gauge undercatch due to strong winds within mesoscale convective systems (MCSs), the underestimate bias ratios could be larger. Q3RAD exhibited a lower RMSE and MAE than Dual Pol for moderately high precipitation amounts; for high precipitation amounts, the results were reversed. Although stage IV and Q3gc precipitation estimates consistently exhibited better results in RMSE and MAE than the three radar-only products, there were some slight inconsistencies. For example, the Q3gc overestimate bias ratio is slightly more than Q3RAD. This was likely the result of comparing Q3gc estimates to 24-h CoCoRaHS gauge totals and the gauge-correction process used in MRMS. Consider an automated gauge and a CoCoRaHS gauge located within 15 km, an arbitrary but sufficient distance, of each other in stratiform rain. The two gauge totals will likely be quite similar because of the typically homogenous distribution of rain in stratiform precipitation events in the absence of terrain. As outlined in Zhang et al. (2016), all the radar-only QPEs within the sphere of influence of the automated gauge will be corrected by the use of the IDW function.

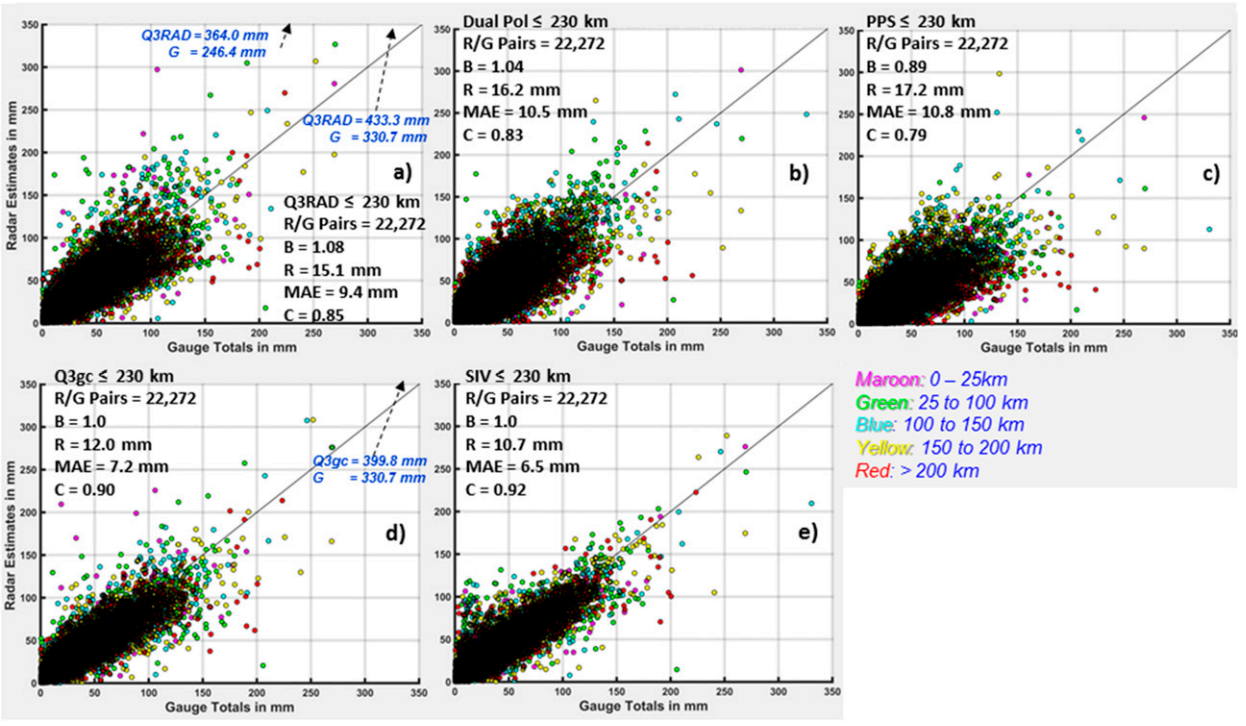

FIG. 3. Comparison between (a) Q3RAD, (b) Dual Pol, (c) PPS, (d) Q3gc, and (e) stage IV estimates vs 24-h totals from CoCoRaHS gauges for all data east of the Rockies and at distances ≤230 km from the radar. *R*/*G* pairs have been color coded according to the image legend. Outliers are denoted by dashed arrows with *R*/*G* values shown in box. One-to-one line is shown in solid black. Legend is as in Fig. 1.

Once done, the gauge-corrected QPE will likely match well to the CoCoRaHS gauge, as both gauges were located in stratiform rain. Now, consider the same situation except the CoCoRaHS gauge was located within convection while the automated gauge remained within stratiform rain. The CoCoRaHS gauge will have a relatively higher hourly total than the automated gauge because of the higher rain rates typically present in convection. The gauge-correction algorithm will use the automated gauge total to reduce totals in the radar-generated QPE within the sphere of influence (where convection was present) via the IDW function. Therefore, when the gauge-corrected QPE is compared to the CoCoRaHS gauge, it will likely result in an underestimate bias ratio. Finally, consider when the automated gauge is located where convection was present but the CoCoRaHS gauge was within stratiform rain. Now, the automated gauge will have a relatively higher hourly total than the CoCoRaHS gauge. In this case, the radar-only QPE within the sphere of influence of the automated gauge will be increased. This means an overestimate bias would result when Q3gc is compared to the CoCoRaHS gauge. Overall, the degradation in bias ratio caused by this type of an effect should be small when adequate numbers of automated gauges are available. This was corroborated by the very small degradation observed when the Q3gc bias ratio was compared to that of Q3RAD (Table 1).

Finally, the stage IV and the Dual Pol estimates had essentially the same bias ratio for both of the higher-precipitation categories; it may seem surprising that the stage IV estimate did not have a significantly better bias ratio than Dual Pol. However, as previously mentioned, stage IV estimates may utilize various radar-only and satellite precipitation estimates. What was important was that the stage IV estimate had significantly lower RMSE and MAE than Dual Pol because of the forecaster input and manually quality-controlled gauge-corrected process. In fact, the overall results shown in Fig. 1 indicated that as a whole the gauge-corrected products performed better than the radar-only products.

It is important to note that time is required to produce stage IV and Q3gc estimates because of the time requirement for the gauge reports to be disseminated, ingested, and for the QC process within the respective algorithms to be completed. Hence, there is a time latency before the gauge-corrected products are delivered to field forecasters. However, Q3RAD, Dual Pol, and PPS estimates are real-time products that are available to forecasters much sooner. Further, the gauge-corrected

TABLE 1. Number of *R*/*G* pairs, radar-to-gauge bias ratio, RMSE, and MAE for Q3RAD, Dual Pol, PPS, Q3gc, and stage IV estimates stratified by 24-h gauge amount. Values in boldface denote the lowest RMSE and MAE results for a given category.

Product	*R*/*G* pairs	Bias	RMSE (mm)	MAE (mm)
$G < 12.7$ mm (0.50 in.)				
Q3RAD	8803	1.69	7.0	4.6
Dual Pol		1.61	7.9	5.0
PPS		1.43	6.7	4.3
Q3gc		1.47	5.7	3.6
Stage IV		1.41	**5.5**	**3.3**
12.7 (0.50) $\leq G <$ 38.1 mm (1.50 in.)				
Q3RAD	8240	1.18	12.2	8.7
Dual Pol		1.11	14.3	10.3
PPS		0.96	12.7	9.6
Q3gc		1.08	9.7	6.5
Stage IV		1.05	**9.1**	**6.2**
38.1 (1.50) $\leq G <$ 101.6 mm (4.00 in.)				
Q3RAD	4667	0.97	21.9	16.4
Dual Pol		0.94	23.6	18.5
PPS		0.80	25.6	20.6
Q3gc		0.93	16.6	12.5
Stage IV		0.93	**14.5**	**10.8**
$G \geq 101.6$ mm (4.00 in.)				
Q3RAD	562	0.83	45.2	36.9
Dual Pol		0.85	42.8	33.2
PPS		0.65	56.3	47.2
Q3gc		0.81	39.5	31.2
Stage IV		0.84	**32.6**	**24.5**

products in a sense are a correction of the radar-only product via the use of QC gauges. Hence, from this point on, our focus will be on the radar-only products and their performance in different geographical regions.

4. Regional statistical analysis and results

a. QPE assessment for southern plains, Southeast/mid-Atlantic, and Northeast

Scatterplots and statistical measures for Q3RAD, Dual Pol, and PPS were further examined for the previously defined five regions. The results for *R*/*G* pairs ≤230 km over the southern plains, Southeast/mid-Atlantic, and Northeast are shown in Fig. 4. Q3RAD exhibited significantly decreased scatter and generally more favorable statistical measures over the southern plains and the Northeast. Q3RAD RMSEs and MAEs were between 16% and 23% lower than Dual Pol for these regions. Over the Southeast/mid-Atlantic, Q3RAD and Dual Pol exhibited similar RMSE and MAE with differences of 1 mm or less, although the former exhibited less scatter. Dual Pol RMSEs and MAEs were approximately 10%–15% lower than PPS over the Northeast and Southeast/mid-Atlantic. Little difference in RMSE and MAE was noted between Dual Pol and PPS over the southern plains. For all three regions, Q3RAD exhibited a slight underestimate bias ratio but was still within 10% of one; the Dual Pol bias ratio was nearly one over the southern plains but exhibited underestimate bias ratios over the Southeast/mid-Atlantic and Northeast. PPS exhibited a distinct underestimate bias ratio for all three regions.

Table 2 showed results for all three regions when *R*/*G* pairs were stratified with respect to the melting layer. Below the melting layer, Q3RAD showed better RMSE and MAE than Dual Pol and PPS. Dual Pol exhibited slightly better RMSE than PPS, although both products had a similar MAE. PPS exhibited a significant underestimate bias ratio while Dual Pol and Q3RAD had bias ratios close to unity. Within and above the melting layer, Q3RAD RMSEs (MAEs) were ~12% and 22% (~14% and 30%) lower than Dual Pol, respectively. These differences reflected the MRMS advantage of using a VPR correction and a reflectivity mosaic. Further, Dual Pol exhibited RMSE (MAE) values that were ~6% and 18% (~6% and 14%) lower than PPS for estimates made within and generally above the melting layer.

One major factor for the large errors in PPS was most likely the single *Z*–*R* relationship, which was often set to the default convective type ($Z = 300R^{1.4}$), did not well represent some warm rain events. The polarimetric radar synthetic QPE in Dual Pol, based on hydrometeor classification (Giangrande and Ryzhkov 2008; Berkowitz et al. 2013) and the adaptive *Z*–*R* relationships in Q3RAD based on precipitation classifications (Zhang et al. 2016), on the other hand, better accounted for the warm rain processes and resulted in less of an underestimation.

It is interesting that the PPS underestimation bias is lower in the melting layer than below or above. This was because inflated reflectivities in the melting layer somewhat compensated the underestimation from an inadequate (underestimating) *Z*–*R* relationship and/or the vertical variations of reflectivity. As a result, the underestimation bias was reduced although for the wrong reason. Above the melting layer, both single-radar QPEs, PPS and Dual Pol, exhibited large underestimation biases because the data used for rain-rate calculations were from the ice region and the estimation was not representative of what reached the ground. Such discrepancies are mainly from 1) vertical variations of hydrometeor phase and drop size distributions and 2) inaccurate relationships between the radar variables, obtained in ice regions, and the liquid water content.

In addition to melting layer and radar sampling challenges, other error factors included calibration biases and partial beam blockage. An example of a Z_{DR}

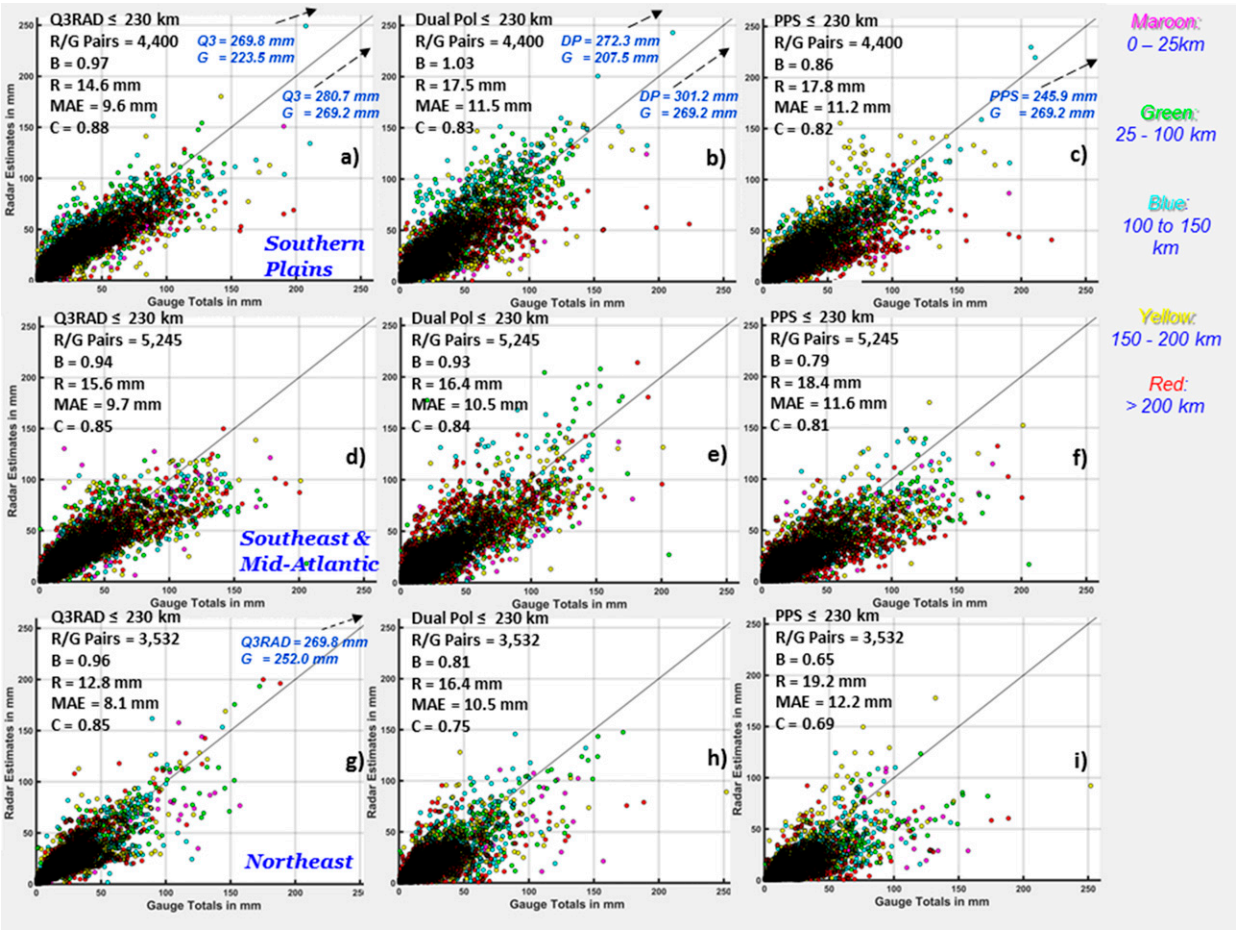

FIG. 4. (left) Q3RAD, (center) Dual Pol, and (right) PPS estimates vs 24-h totals from CoCoRaHS gauges. The results are from the (top) southern plains, (middle) Southeast/mid-Atlantic, and (bottom) Northeast. Legend is as in Fig. 1.

calibration issue and its impact on the Dual Pol QPE was illustrated in Fig. 5. During the precipitation event, the KEWX (Austin, Texas) radar exhibited a negative Z_{DR} bias; comparison with neighboring radars suggested the mean offset was ~0.40 dB. This negative Z_{DR} bias resulted in a significant overestimation bias in the Dual Pol estimate (green and blue circles in Fig. 5) where the $R(Z, Z_{DR})$ relationship was applied since the rain rate was proportional to $Z_{DR}^{-3.43}$ (Giangrande and Ryzhkov 2008). The Z_{DR} accuracy is expected to improve as the Radar Operations Center (ROC) continues to develop ways to mitigate the Z_{DR} calibration error (Zittel et al. 2015).

Figure 6 illustrates the effects of partial blockage and brightband impacts on single-radar QPEs. Figure 6 showed 24-h accumulations and radar estimate versus gauge scatterplots for PPS and Dual Pol for a rainfall event that passed over the KGYX (Portland, Maine) radar on 13 and 14 August 2014. This particular precipitation event was one that affected portions of the mid-Atlantic and Northeast coast over a 2-day period and was associated with substantial rainfall totals, some over 200 mm (8.0 in.), reminiscent of tropical-like rainfall events. Partial beam blockage was clearly seen in both PPS and Dual Pol QPEs south and southeast of the radar (Figs. 6a–b) where many of the higher underestimates (warm-colored bubbles) were found. The strong underestimation was also apparent in the scatterplots of PPS (Fig. 6c) and Dual Pol (Fig. 6d) versus gauges, except for some points within the brightband areas. Overall, the Dual Pol estimates exhibited less of an underestimate bias ratio and lower RMSE and MAE than PPS. In turn, Q3RAD (not shown) had a lower underestimate bias ratio (50% less) and lower RMSE (25%) and MAE (30%) than Dual Pol. New techniques using specific attenuation $R(A)$ (Ryzhkov et al. 2014; Wang et al. 2014) have shown great potential in mitigating radar QPE underestimates in partial beam blockage, and the operational MRMS radar-only QPE is expected to be upgraded with the new techniques by the warm season of 2017.

TABLE 2. Number of *R*/*G* pairs, radar-to-gauge bias ratio, RMSE, and MAE for Q3RAD, Dual Pol, and PPS estimates made below, generally within, and near the top or above the melting layer for all the precipitation events found within the southern plains, Southeast/mid-Atlantic, and Northeast. Values in boldface denote the lowest RMSE and MAE results for a given category.

Product	*R*/*G* pairs	Bias	RMSE (mm)	MAE (mm)
Below melting layer				
Q3RAD	5261	1.00	**15.0**	**9.7**
Dual Pol		0.93	16.4	10.3
PPS		0.79	17.1	10.5
Within melting layer				
Q3RAD	5030	0.93	**14.1**	**9.0**
Dual Pol		0.94	16.0	10.5
PPS		0.88	17.0	11.2
Near top of or above melting layer				
Q3RAD	2886	0.91	**14.5**	**8.8**
Dual Pol		0.92	18.7	12.5
PPS		0.61	22.7	14.5

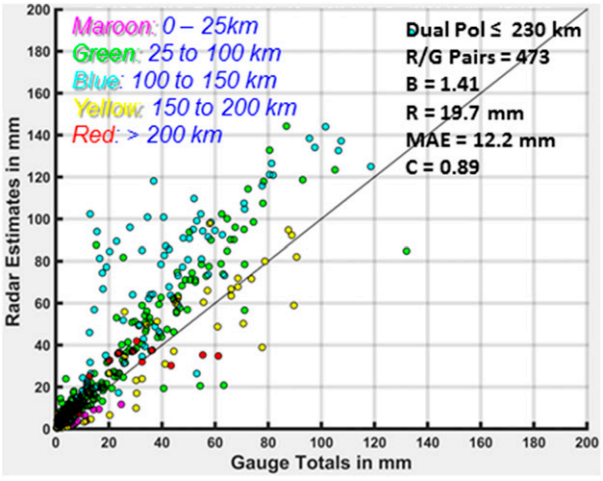

FIG. 5. Dual Pol estimates vs 24-h totals from CoCoRaHS gauges for the 24-h period ending at 1200 UTC 26 May 2014. The data collected were centered upon the KEWX WSR-88D. Legend is as in Fig. 1.

b. *QPE assessment for Great Lakes/Midwest and northern/central plains*

Figure 7 shows the QPE assessment for the Great Lakes/Midwest and northern/central plains. In both regions, Q3RAD had a tighter grouping of data than both Dual Pol and PPS for precipitation totals <75 mm; however, Q3RAD also exhibited more of an overestimate bias than both Dual Pol and PPS. Over the Great Lakes/Midwest region, Q3RAD, Dual Pol, and PPS RMSE and MAE differences all were within 1 mm of each other, although PPS exhibited appreciably more scatter. PPS had the best bias ratio in both regions and it exhibited lower RMSEs and MAEs in the northern/central plains. This result indicated that the default Z–R relationship ($Z = 300R^{1.4}$) often used in PPS well represented the drop size distribution in most of the precipitation systems observed in the northern/central plains within this study.

Table 3 showed the radar-only product performance for both geographical regions segregated by the melting layer. Q3RAD exhibited a large wet bias ratio in each category due to a potential overclassification of tropical rain, a topic to be discussed shortly. Both PPS and Dual Pol performed significantly better than Q3RAD below the melting layer, with ~30% lower RMSE and MAE. In the melting layer, there was a notable overestimation bias for both Dual Pol and PPS, a contrast to what was observed the southern plains, Southeast/mid-Atlantic, and Northeast. Q3RAD performed significantly better than Dual Pol and PPS with at least ~20% lower RMSE and MAE. This was probably due to lower melting layers and more intense bright bands at these higher latitudes causing artificially inflated rain rates in PPS that did not have a brightband correction for reflectivity. Dual Pol mitigates the impact of the bright band on QPE by using the multiplication factors of 0.6 and 0.8 applied to the default convective Z–R relationship for hydrometeor classifications of wet snow and graupel, respectively. However, this correction was not able to account for the spatial variations in the brightband intensity. An example of Dual Pol QPE overestimation associated with the melting layer is shown in Fig. 8. Hourly Dual Pol QPE from KOAX (Omaha, Nebraska) ending at 0300 UTC 4 June 2014 showed a number of overestimates with respect to gauges (i.e., the blue dots in the yellow oval, Fig. 8a) northeast of the radar, where Dual Pol correlation coefficient (not shown) clearly indicated the existence of the melting layer. The melting layer character was also apparent in the KOAX reflectivity at 0230 UTC (Fig. 8b, red oval), which was at least 5.0 dBZ higher than KDMX (Des Moines, Iowa) observations (Fig. 8c, red oval). Another contributing factor to the overestimation was calibration bias. Using the same method used in Cocks et al. (2016), the calibration between KOAX in the equidistant regions to its neighboring radars revealed a positive bias between 1.0 and 1.5 dBZ in KOAX. Such a calibration bias would have an impact on the Q3RAD and PPS estimates as well.

For estimates above the melting layer, Q3RAD exhibited ~7% (~5%) lower RMSE (MAE) than PPS. Further, PPS exhibited a ~19% (~24%) lower RMSE (MAE) than Dual Pol. The higher Dual Pol QPE error was likely related to an empirical relationship of 2.8 times the default convective Z–R relationship applied

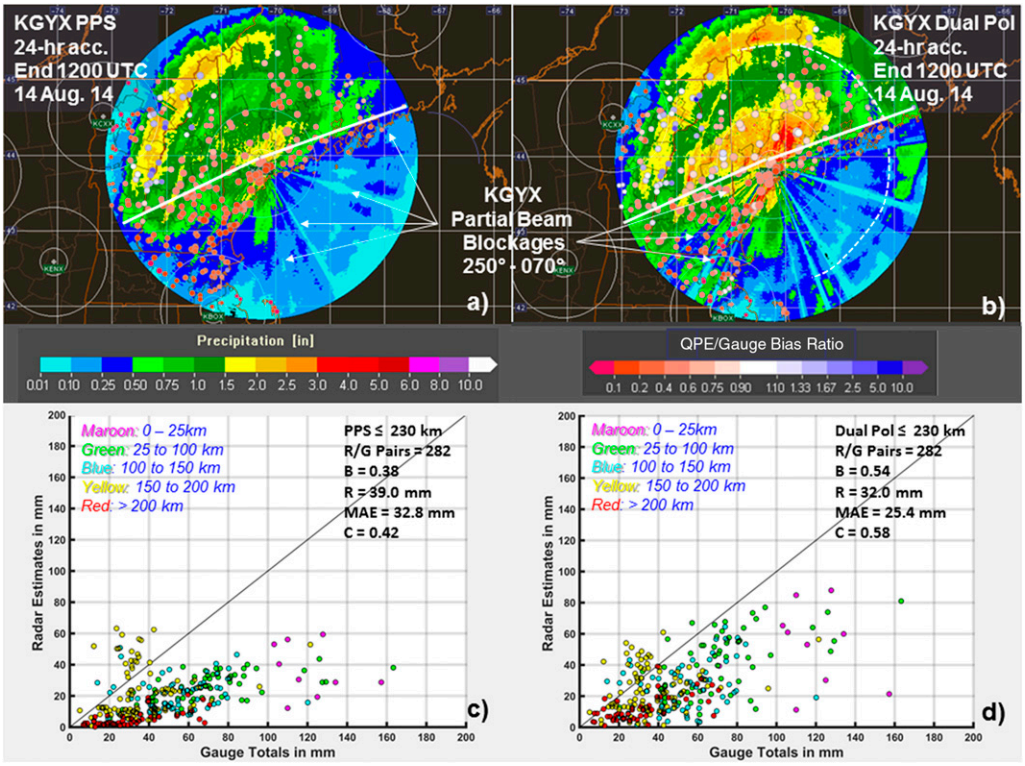

FIG. 6. The 24-h accumulation of (a) PPS and (b) Dual Pol QPE and accompanying radar estimate vs 24-h gauge totals scatterplots for (c) PPS and (d) Dual Pol for the period ending at 1200 UTC 14 Aug 2014. In (a) and (b), solid white lines denote span of partial blockage around KGYX. Dashed white lines in (b) denote the artificial boundaries created by the different methods the Dual Pol QPE algorithm calculates QPE within and above the melting layer.

above the top of the melting layer. The large overestimation resulted in discontinuities that were frequently observed in the top of the melting layer. An example of this can be seen along the white dashed circle in Fig. 6b, and this discontinuity between estimates within and above the melting layer is discussed in Berkowitz et al. (2013). The ROC released software build 15.0 to the WSR-88D field in the spring of 2015 in order to mitigate this overestimate tendency by 1) changing some of the logic defining the top of the melting layer and 2) giving forecasters the option to adjust the application factor (default = 2.8) above the top of the melting layer to a value considered more representative (Warning Decision Training Branch 2014).

Since a large percentage of the precipitation events in the Great Lakes/Midwest and northern/central plains had vigorous convection, some of the overestimate bias observed in Q3RAD and Dual Pol estimates were likely due to wind-induced gauge undercatch (Wilson and Brandes 1979; Neff 1977; Sieck et al. 2007) as well as hail contaminating reflectivity data. However, closer examination indicated some of the Q3RAD overestimation was due to factors other than hail or high wind. Figure 9 showed the 24-h Q3RAD precipitation estimates ending at 1200 UTC 28 August 2014. There were no reports of hail or high winds from Storm Prediction Center local storm reports or the Meteorological Phenomena Identification Near the Ground (mPING) project (Elmore et al. 2014). Further, synoptic observations (not shown) for the 24-h period indicated winds were mostly $\leq 5\,\mathrm{m\,s^{-1}}$, although two stations indicated gusts to $10\,\mathrm{m\,s^{-1}}$ with convection for one hourly observation. Therefore, errors due to hail contamination and gauge undercatch should be relatively insignificant. Yet, Q3RAD exhibited an overestimate bias ratio (2.17) with RMSE (MAE) of 51.9 mm (37.2 mm). Given the maximum observed winds of $5–10\,\mathrm{m\,s^{-1}}$, the gauge undercatch should be around 4%–10% (Duchon and Essenberg 2001; Sieck et al. 2007); therefore, this factor could not account for all the overestimation observed with Q3RAD. Further, the KOAX radar reflectivity was generally within 1 dBZ of its neighboring radars so calibration error could not account for error as well. An analysis of the MRMS surface precipitation type indicated that the primary classes identified were tropical stratiform or tropical convective for the hours with the largest errors. The model data–derived probability of

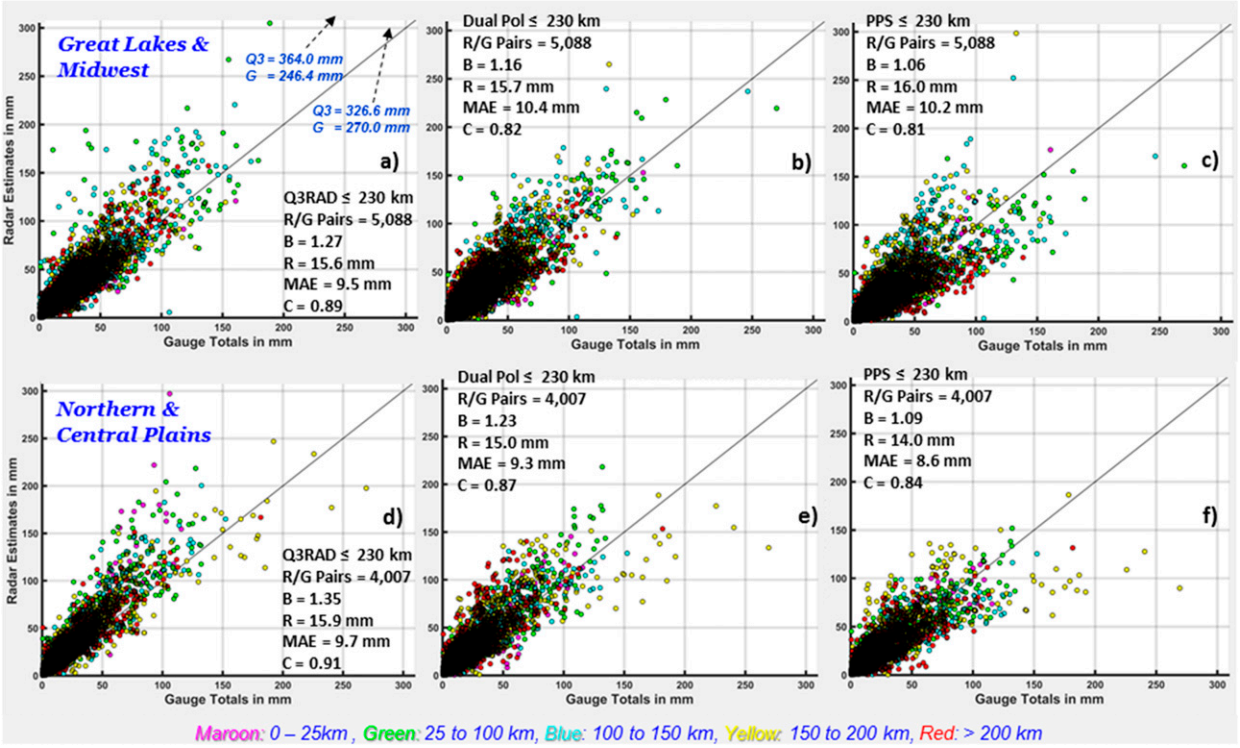

FIG. 7. (a),(d) Q3RAD; (b),(e) Dual Pol; and (c),(f) PPS estimates vs 24-h CoCoRaHS gauge totals for the (top) Great Lakes/Midwest and (bottom) northern/central plains. Legend is as in Fig. 1.

warm rain (POWR; Zhang et al. 2016) had values generally >0.8 within the region. As a result, the tropical Z–R relationship with an enhancing factor greater than 1.0 was applied even though the actual precipitation was more continental convective in nature. Such misclassifications were observed in other events and were a major contributor to the Q3RAD overestimation in the northern/central plains and Great Lakes/Midwest during the warm season. In many events identified as tropical, some gauges (especially in the warm and moist sections) did exhibit high rainfall totals, while many others did not support the predominance of tropical convection. The difference indicated high spatial variabilities of drop size distributions in summertime MCSs at higher latitudes and the deficiency of the Q3RAD precipitation classification based on mean vertical profiles of reflectivity (Xu et al. 2008) and POWR (Grams et al. 2014) in capturing such variabilities.

An adjustment to the Q3RAD tropical rain-rate relationship was recently developed to mitigate the large wet bias in the central and northern continental United States. The adjustment is applied to the empirical enhancing factor $\alpha_{\max}$ that Q3RAD used to boost tropical rain rates. Factor $\alpha_{\max}$ is a function of time (Fig. 10a) based on Atlantic tropical cyclone climatology with values of 1.0 between December and May, but increases during the hurricane season to a peak value of 1.5 by mid-September. This factor was applied to tropical precipitation over the contiguous United States east of 100°W (Zhang et al. 2016) regardless of latitudes or the proximity to the ocean. However, Parameter-Elevation Regressions on Independent Slopes Model (PRISM; Daly et al. 2008, 1994; www.prism.oregonstate.edu) precipitation climatology, tropical cyclone track

TABLE 3. As in Table 2, but for events found within the northern/central plains and Great Lakes/Midwest.

Product	*R*/*G* pairs	Bias	RMSE (mm)	MAE (mm)
Below melting layer				
Q3RAD	3026	1.33	20.7	12.2
Dual Pol		1.06	**13.6**	**8.3**
PPS		1.00	14.8	9.6
Within melting layer				
Q3RAD	4042	1.27	**12.7**	**8.4**
Dual Pol		1.32	16.3	10.5
PPS		1.22	16.4	9.8
Near top of or above melting layer				
Q3RAD	2027	1.28	**12.2**	**8.2**
Dual Pol		1.39	16.1	11.3
PPS		0.93	13.1	8.6

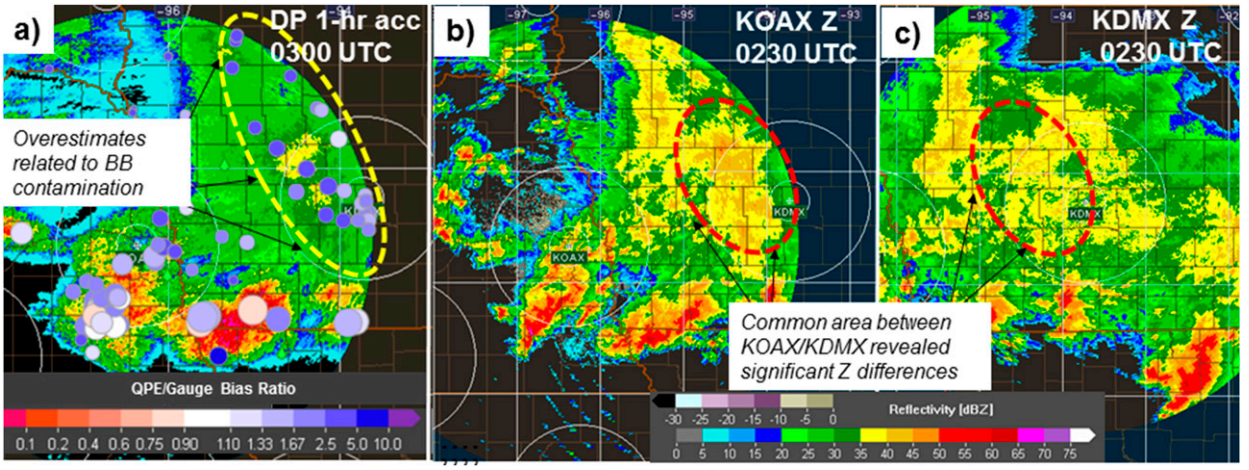

FIG. 8. (a) KOAX 0300 UTC Dual Pol 1-h accumulations along with (b) KOAX and (c) KDMX digital hybrid scan reflectivity at 0230 UTC 4 Jun 2014. In (a), the region of overestimates within the melting layer was denoted by the dashed yellow oval. For (b) and (c), the common region between both KOAX and KDMX is outlined in red.

history, and CoCoRaHS extreme daily precipitation distributions for totals >279 mm (11.0 in.; N. Doesken 2016, personal communication) all indicated the highest risk of heavy tropical rainfall being over the southern United States and coastal areas. To account for the spatial variations of the likelihood of heavy tropical rain, a new tropical rain rate enhancing factor $\alpha'_{\max}$ was calculated:

$$\alpha'_{\max} = 1.0 + f(\alpha_{\max} - 1), \quad (1)$$

where f is a spatial variability factor as shown in Fig. 10b. Figures 11a and 11b show 24-h Q3RAD estimates made with the old and new $\alpha_{\max}$ from precipitation events in the northern/central plains and Great Lakes/Midwest between July and October 2014 and their comparisons with quality-controlled CoCoRaHS and automated gauges, a total of 6827 *R*/*G* pairs. The *R*/*G* pairs selected were those in which a tropical classification was made during the 24-h period and were primarily located in the region where the f reduction factor was <0.2. The results clearly showed improved performance with the MAE reduced by ~22% and the overestimation bias ratio reduced by ~8.0%. This improvement was implemented in the operational MRMS system in the fall of 2016.

Aside from the tropical rain rate enhancing factor adjustment, recent efforts in the radar QPE using specific attenuation derived from Dual Pol radar observations showed good potential in better representing drop size distributions and in reducing QPE errors (Ryzhkov et al. 2014; Wang et al. 2014). A new synthetic MRMS

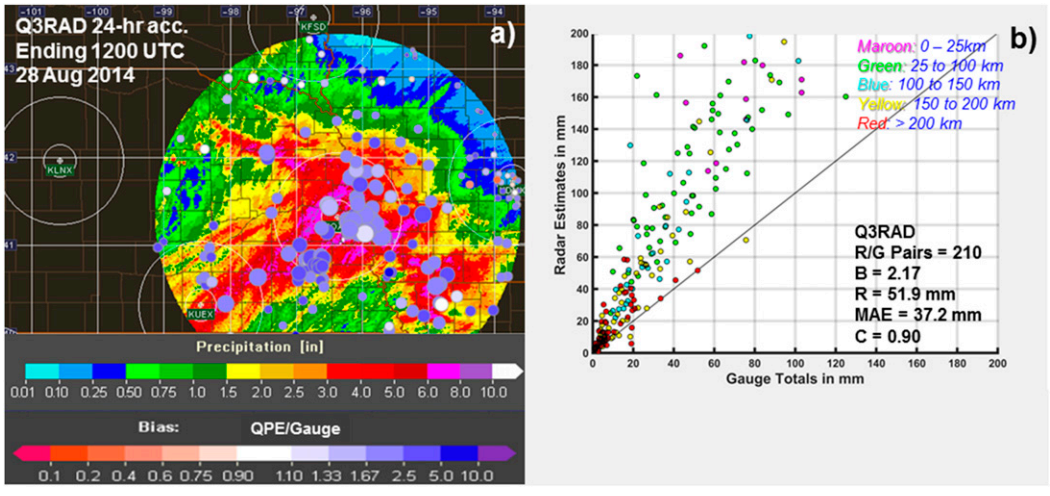

FIG. 9. (a) Q3RAD 24-h QPE accumulations with gauge-to-radar estimate bias bubbles and (b) the radar estimate vs gauge scatterplot for the period ending at 1200 UTC 28 Aug 2014. The statistical measures legend is as in Fig. 1.

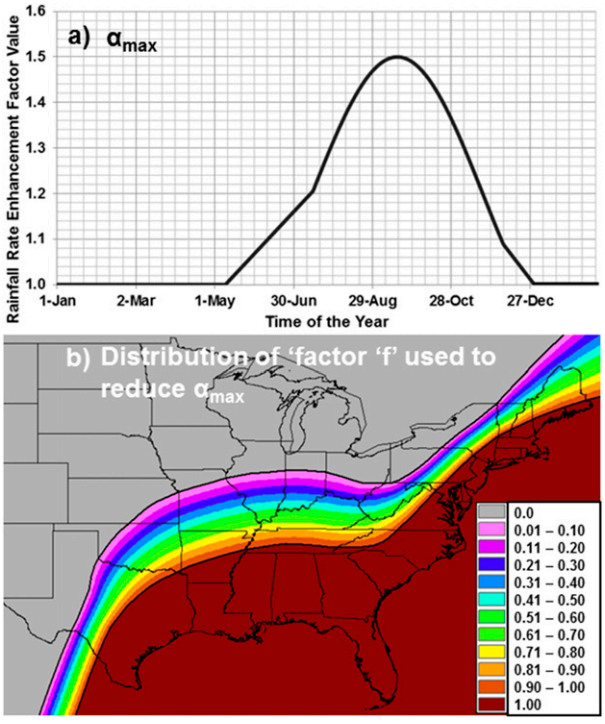

FIG. 10. (a) The value of the tropical rain-rate enhancing factor (i.e., α_{max}) as a function of calendar date and (b) the gridded values of the factor f used to reduce the portion of $\alpha_{max} > 1.0$.

radar QPE based on $R(A)$, $R(K_{DP})$, and $R(Z)$ is currently under evaluation and has shown the potential to further improve warm season precipitation estimation in the eastern United States.

5. Conclusions

Examination of 2014 warm season precipitation events east of the Rocky Mountains showed that Q3RAD exhibited lower error and higher correlation with respect to the validation gauges than Dual Pol, although the differences between products were smaller than seen during the previous cool season. Both products performed better than PPS. The improved Dual Pol performance was due to higher freezing levels and deeper precipitation systems, and thus more usage of $R(Z, Z_{DR})$ and $R(K_{DP})$ relationships that better capture drop size distributions than $R(Z)$ with empirical multiplier factors. The forecaster quality-controlled NCEP stage IV estimates that integrated radar, gauge, satellite, and precipitation climatology outperformed the real-time radar-only products as expected. While stage IV estimates showed less scatter and lower errors than MRMS Q3gc, the performance of the latter was remarkable considering it was an automated product available hourly with potentially shorter delays. However, because of the manual QC associated with stage IV precipitation analysis, these should continue to be considered the standard for which all other quantitative precipitation estimates are made.

Precipitation estimates stratified by 24-h gauge totals indicated that all of the products exhibited an overestimate bias ratio for light precipitation, likely due to precipitation evaporating before reaching the gauge and gauge wetting losses. For gauge totals >101.6 mm (4.00 in.), all of the products exhibited an underestimate bias ratio indicating deficiencies in all the QPEs to accurately capture the heavy rain microphysical processes.

A regional analysis was performed using the three radar-only products: Q3RAD, Dual Pol, and PPS. Scatterplot analysis and stratification of errors for R/G pairs below, within, and generally above the melting layer indicated Q3RAD performed better than single-radar QPEs over the southern plains, Southeast/mid-Atlantic, and Northeast. In general,

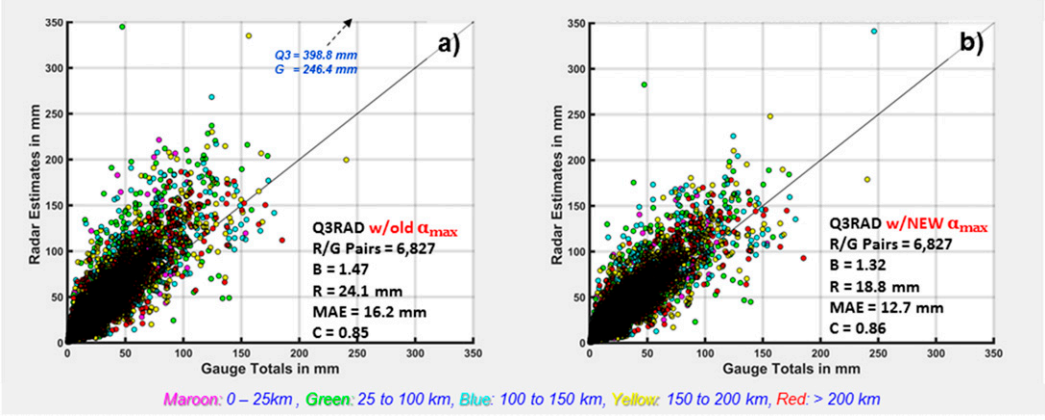

FIG. 11. (a) Q3RAD calculated using the previous version of α_{max} and (b) Q3RAD calculated using the new α_{max} as compared to 24-h gauge totals.

Dual Pol exhibited better performance than PPS. Overall, the larger Q3RAD improvements were observed within and above the melting layer.

Over the northern/central plains and the Great Lakes/Midwest, both Dual Pol and PPS showed better performance than Q3RAD below the melting layer. Q3RAD had a large overestimate bias ratio due to Q3RAD often classifying radar echoes within MCSs as tropical and an enhanced empirical rain-rate relationship was applied. An adjustment was made to the rainfall enhancing factor and resulted in ~22% reduction in MAE and a ~15.5% reduction in the bias ratio. Work continues on refining MRMS precipitation classification to minimize the incorrect tropical rain identification in the aforementioned regions.

Within and above the melting layer, Q3RAD had fewer errors than Dual Pol and PPS despite the precipitation type classification issue. Dual Pol, on the other hand, showed relatively large overestimate biases within and above the melting layer due to a simplistic brightband-correction scheme that could not account for variations of the brightband intensity. Much of the overestimate bias observed for Dual Pol was located within and above the melting layer. Calibration errors were another factor that impacted the three radar QPEs. All three products were likely impacted by gauge undercatch due to strong winds and hail contamination given the sizable number of severe storm events evaluated in the northern/central plains and Great Lakes/Midwest. Overall, Q3RADs better performance within and above the melting layer can be attributed to the use of a reflectivity mosaic with a vertical profile reflectivity correction for brightband contamination.

Future work for the Dual Pol QPE includes improving the melting layer detection and HHC algorithms, as well as developing QPE that is not as dependent upon Z or Z_{DR} calibration. For MRMS, a dual-polarization radar synthetic QPE using $R(A)$, $R(K_{DP})$, and $R(Z)$ is under development which aims at making estimates using a combination of $R(A)$ in widespread rain, $R(K_{DP})$ in areas of hail and Q3RAD $R(Z)$ elsewhere. Initial results will be reported in an upcoming paper.

Acknowledgments. We thank Alexander Ryzhkov and Dusan Zrnić for providing many useful comments that improved the manuscript. Funding was provided by NOAA/Office of Oceanic and Atmospheric Research under NOAA–University of Oklahoma Cooperative Agreement NA11OAR4320072, U.S. Department of Commerce, as well as the Radar Operations Center technical transfer memorandum of agreement.

REFERENCES

Berkowitz, D. S., J. A. Schultz, S. Vasiloff, K. L. Elmore, C. D. Payne, and J. B. Boettcher, 2013: Status of dual pol QPE in the WSR-88D network. *27th Conf. on Hydrology,* Austin, TX, Amer. Meteor. Society, 2.2. [Available online at https://ams.confex.com/ams/93Annual/webprogram/Paper221525.html.]

Cocks, S., S. Martinaitis, B. Kaney, J. Zhang, and K. Howard, 2016: MRMS QPE performance during the 2013/14 cool season. *J. Hydrometeor.*, **17**, 791–810, doi:10.1175/JHM-D-15-0095.1.

Daly, C. R., P. Neilson, and D. L. Phillips, 1994: A statistical–topographic model for mapping climatological precipitation over mountainous terrain. *J. Appl. Meteor.*, **33**, 140–158, doi:10.1175/1520-0450(1994)033<0140:ASTMFM>2.0.CO;2.

——, M. Halbleib, J. Smith, W. Gibson, M. Doggett, G. Taylor, J. Curtis, and P. Pasteris, 2008: Physiographically sensitive mapping of climatological temperature and precipitation across the conterminous United States. *Int. J. Climatol.*, **28**, 2031–2064, doi:10.1002/joc.1688.

Doviak, R. J., and D. S. Zrnić, 2006: *Doppler Radar and Weather Observations.* 2nd ed. Dover Publications, 592 pp.

Droegemeier, K. K., and Coauthors, 2000: Hydrological aspects of weather prediction and flood warnings. Report on the 9th prospectus development team of the U.S. Weather Research Program. *Bull. Amer. Meteor. Soc.*, **81**, 2665–2680, doi:10.1175/1520-0477(2000)081<2665:HAOWPA>2.3.CO;2.

Duchon, C. E., and G. R. Essenberg, 2001: Comparative rainfall observations from pit and aboveground rain gauges with and without wind shields. *Water Resour. Res.*, **37**, 3253–3263, doi:10.1029/2001WR000541.

Elmore, K. L., Z. L. Flamig, V. Lakshmanan, B. T. Kaney, V. Farmer, H. D. Reeves, and L. P. Rothfusz, 2014: MPING: Crowd-sourcing weather reports for research. *Bull. Amer. Meteor. Soc.*, **95**, 1335–1342, doi:10.1175/BAMS-D-13-00014.1.

Fiebrich, C. A., C. R. Morgan, A. G. McCombs, P. K. Hall, and R. A. McPherson, 2010: Quality assurance procedures for mesoscale meteorological data. *J. Atmos. Oceanic Technol.*, **27**, 1565–1582, doi:10.1175/2010JTECHA1433.1.

Fulton, R., J. Breidenbach, D. Seo, D. Miller, and T. O'Bannon, 1998: The WSR-88D rainfall algorithm. *Wea. Forecasting*, **13**, 377–395, doi:10.1175/1520-0434(1998)013<0377:TWRA>2.0.CO;2.

Giangrande, S., and A. Ryzhkov, 2008: Estimation of rainfall based on the results of polarimetric echo classification. *J. Appl. Meteor.*, **47**, 2445–2462, doi:10.1175/2008JAMC1753.1.

Grams, H., J. Zhang, and K. Elmore, 2014: Automated identification of enhanced rainfall rates using the near-storm environment for radar precipitation estimates. *J. Hydrometeor.*, **15**, 1238–1254, doi:10.1175/JHM-D-13-042.1.

Groisman, P. Ya., and D. R. Legates, 1994: The accuracy of United States precipitation data. *Bull. Amer. Meteor. Soc.*, **75**, 215–227, doi:10.1175/1520-0477(1994)075<0215:TAOUSP>2.0.CO;2.

Kim, D., B. Nelson, and D. J. Seo, 2009: Characteristics of reprocessed Hydrometeorological Automated Data System (HADS) hourly precipitation data. *Wea. Forecasting*, **24**, 1287–1296, doi:10.1175/2009WAF2222227.1.

Krajewski, W. F., G. Villarini, and J. A. Smith, 2010: Radar–rainfall uncertainties: Where are we after thirty years of effort? *Bull. Amer. Meteor. Soc.*, **91**, 87–94, doi:10.1175/2009BAMS2747.1.

Kumjian, M. R., 2013: Principles and applications of dual-polarization weather radar. Part II: Warm- and cold-season applications. *J. Oper. Meteor.*, **1**, 243–264, doi:10.15191/nwajom.2013.0120.

Martinaitis, S. M., 2008: Effects of multi-sensor radar and rain gauge data on hydrologic modeling in relatively flat terrain. M. S. thesis, Dept. of Meteorology, Florida State University, 99 pp. [Available online at http://diginole.lib.fsu.edu/islandora/object/fsu%3A180955 .]

Marzen, J., and H. E. Fuelberg, 2005: Developing a high resolution precipitation dataset for Florida hydrologic studies. *19th Conf. on Hydrology*, New Orleans, LA, Amer. Meteor. Soc., J9.2. [Available online at https://ams.confex.com/ams/Annual2005/techprogram/paper_83718.htm.]

Neff, E. L., 1977: How much rain does a rain gage gage? *J. Hydrol.*, **35**, 213–220, doi:10.1016/0022-1694(77)90001-4.

Nelson, B., O. Prat, D. Seo, and E. Habib, 2016: Assessment and implications of NCEP stage IV quantitative precipitation estimates for product comparisons. *Wea. Forecasting*, **31**, 371–394, doi:10.1175/WAF-D-14-00112.1.

Rinehart, R. E., 2010: *Radar for Meteorologists.* 5th ed. Department of Atmospheric Sciences, University of North Dakota, 150–158.

Ryzhkov, A. V., M. Diederich, P. Zhang, and C. Simmer, 2014: Potential utilization of specific attenuation for rainfall estimation, mitigation of partial beam blockage, and radar networking. *J. Atmos. Oceanic Technol.*, **31**, 599–619, doi:10.1175/JTECH-D-13-00038.1.

Sieck, L. C., S. J. Burges, and M. Steiner, 2007: Challenges in obtaining reliable measurements of point rainfall. *Water Resour. Res.*, **43**, W01420, doi:10.1029/2005WR004519.

Smith, J. A., D. J. Seo, M. L. Baeck, and M. D. Hudlow, 1996: An intercomparison study of NEXRAD precipitation estimates. *Water Resour. Res.*, **32**, 2035–2046, doi:10.1029/96WR00270.

Steiner, M., J. A. Smith, S. J. Burges, C. V. Alonso, and R. W. Darden, 1999: Effect of bias adjustment and rain gauge data quality control on radar rainfall estimation. *Water Resour. Res.*, **35**, 2487–2503, doi:10.1029/1999WR900142.

Wang, Y., P. Zhang, A. Ryzhkov, J. Zhang, and P. Chang, 2014: Utilization of specific attenuation for tropical rainfall estimation in complex terrain. *J. Hydrometeor.*, **15**, 2250–2266, doi:10.1175/JHM-D-14-0003.1.

Wardlow, B. D., M. C. Anderson, and J. P. Verdin, Eds., 2012: *Remote Sensing of Drought: Innovative Monitoring Approaches*. CRC Press, 484 pp.

Warning Decision Training Branch, 2014: RDA/RPG build 15.0 training. Tech. Doc., version 1411, 12 pp. [Available online at http://www.wdtb.noaa.gov/buildTraining/Build15/documents/Build15-Deploy.pdf.]

Wilson, J. W., and E. A. Brandes, 1979: Radar measurement of rainfall: A summary. *Bull. Amer. Meteor. Soc.*, **60**, 1048–1058, doi:10.1175/1520-0477(1979)060<1048:RMORS>2.0.CO;2.

Xu, X., K. Howard, and J. Zhang, 2008: An automated radar technique for the identification of tropical precipitation. *J. Hydrometeor.*, **9**, 885–902, doi:10.1175/2007JHM954.1.

Zhang, J., and Y. Qi, 2010: A real-time algorithm for the correction of bright band effects in radar-derived QPE. *J. Hydrometeor.*, **11**, 1157–1171, doi:10.1175/2010JHM1201.1.

——, and Coauthors, 2011: National Mosaic and Multi-Sensor QPE (NMQ) system: Description, results, and future plans. *Bull. Amer. Meteor. Soc.*, **92**, 1321–1338, doi:10.1175/2011BAMS-D-11-00047.1.

——, Y. Qi, K. Howard, C. Langston, and B. Kaney, 2012: Radar Quality Index (RQI)—A combined measure for beam blockage and VPR effects in a national network. *IAHS Publ.*, **351**, 388–393.

——, and Coauthors, 2014: Initial operating capabilities of quantitative precipitation estimation in the Multi-Radar Multi-Sensory system. *28th Conf. of Hydrology*, Atlanta, GA, Amer. Meteor. Society, 5.3. [Available online at https://ams.confex.com/ams/94Annual/webprogram/Paper240487.html.]

——, and Coauthors, 2016: Multi-Radar Multi-Sensor (MRMS) quantitative precipitation estimation: Initial operating capabilities. *Bull. Amer. Meteor. Soc.*, **97**, 621–638, doi:10.1175/BAMS-D-14-00174.1.

Zittel, W. D., R. R. Lee, L. M. Richardson, J. G. Cunningham, J. A. Schultz, and R. L. Ice, 2015: Geographical and seasonal availability of light rain, dry snow and Bragg scatter to estimate WSR-88D Z_{DR} system bias. *31st Conf. on Environmental Information Processing Technologies*, Phoenix, AZ, Amer. Meteor. Soc., 11.2. [Available online at https://ams.confex.com/ams/95Annual/webprogram/Paper265374.html.]